

# Comparison of saddle-shape flexibility and elliptical-shape stability between Cosgrove-Edwards and Memo-3D annuloplasty rings using three-dimensional analysis software

Akira Tsuneto<sup>1</sup> · Kiyoyuki Eishi<sup>2</sup> · Takashi Miura<sup>2</sup> · Kazuyoshi Tanigawa<sup>2</sup> · Seiji Matsukuma<sup>2</sup> · Takako Minami<sup>1</sup> · Yuji Koide<sup>1</sup> · Satoshi Ikeda<sup>1</sup> · Hiroaki Kawano<sup>1</sup> · Koji Maemura<sup>1</sup>

Received: 1 February 2016 / Accepted: 24 March 2016 / Published online: 6 April 2016  
© The Japanese Association for Thoracic Surgery 2016

## Abstract

**Objective** To compare three-dimensional dynamics between implanted Cosgrove-Edwards and Sorin Memo-3D annuloplasty rings during the cardiac cycle.

**Methods** We examined 11 Cosgrove-Edwards rings and 20 Sorin Memo-3D rings after mitral plasty using real-time three-dimensional transesophageal echocardiography. We evaluated ring height, ellipticity, and geometry during one cardiac cycle. Four evenly spaced phases each selected during systole and diastole were assessed using REAL VIEW software.

**Results** The height of the Cosgrove-Edwards and Sorin Memo-3D rings was similar ( $2.3 \pm 0.8$  vs.  $1.9 \pm 0.9$  mm,  $p = 0.44$ ). The maximum difference in ring height during one cardiac cycle (change in height) was larger for the Cosgrove-Edwards than the Sorin Memo-3D rings ( $2.3 \pm 0.8$  vs.  $1.5 \pm 0.6$  mm,  $p = 0.014$ ). Ellipticity and the maximum difference in ellipticity during one cardiac cycle (change in ellipticity) were larger for Cosgrove-Edwards than Sorin Memo-3D rings ( $80.0 \pm 9.1$  vs.  $72.0 \pm 4.8$  %,  $p = 0.014$ , respectively, and  $12.0 \pm 3.1$  vs.  $6.0 \pm 1.8$  %,  $p < 0.001$ ).

**Conclusions** Cosgrove-Edwards rings were more flexible, whereas Sorin Memo-3D rings maintained the elliptical shape more effectively.

**Keywords** Cosgrove-Edwards annuloplasty ring · Memo-3D annuloplasty ring · Three-dimensional transesophageal echocardiography · Mitral annular dynamics · Mitral repair

## Introduction

The anatomical shape of the mitral valve annulus of the human heart resembles that of a horse saddle [1, 2], and modern artificial rings for mitral annuloplasty approximate this shape. The three-dimensional (3D) geometry of the human mitral annulus changes with the cardiac cycle [3–5] and thus current artificial rings for mitral annuloplasty are also manufactured such that their 3D geometry changes after surgical implantation. However, the 3D geometric changes among different types of implanted artificial rings have not been fully investigated. Cosgrove-Edwards annuloplasty rings (Edwards Lifesciences, Irvine, CA, USA) are flexible semi-closed loops, and Sorin Memo-3D annuloplasty rings (Sorin Biomedica Cardio S.r.l., Saluggia, Italy) are semi-rigid fully closed annuloplasty loops in which the anterior side is semi-rigid and the posterior side is semi-flexible. The present study compares the 3D geometric changes between implanted Cosgrove-Edwards and Sorin Memo-3D annuloplasty rings during one cardiac cycle after surgery to treat mitral regurgitation (MR).

## Methods

The Ethics Committee at Nagasaki University Hospital approved the protocol for this study, which proceeded according to the Declaration of Helsinki (approval number 16020819).

✉ Akira Tsuneto  
atsuneto@nagasaki-u.ac.jp

<sup>1</sup> Department of Cardiovascular Medicine, Nagasaki University Hospital, 1-7-1 Sakamoto, Nagasaki 852-8501, Japan

<sup>2</sup> Department of Cardiovascular Surgery, Nagasaki University Hospital, 1-7-1 Sakamoto, Nagasaki 852-8501, Japan

## Patients

This study included patients (male,  $n = 15$ ; female,  $n = 16$ ; average age,  $67.2 \pm 15.4$  years; average body surface area,  $1.60 \pm 0.23$  m<sup>2</sup>) [2] (Table 1) who underwent mitral plasty to treat MR (caused by degenerative changes) and from whom we could acquire sufficiently clear 3D-transesophageal echocardiography (3D-TEE) images at the Department of Cardiovascular Surgery, Nagasaki University Hospital between February 2012 and February 2014. Mitral plasty was achieved by resection suturing, chorda reconstruction, and annuloplasty [6]. Eleven Cosgrove-Edwards (Cosgrove) and 20 Sorin Memo-3D (Memo-3D) annuloplasty rings were surgically implanted and the average size of all rings was  $29.0 \pm 1.5$  mm (Table 1). The first operator selected Cosgrove rings for patients with posterior leaflet prolapse, and Memo-3D rings for those with anterior leaflet prolapse, annular dilation, and infective endocarditis with leaflet perforation.

## Echocardiography

The patients were assessed by 3D-TEE using iE33 ultrasound equipment (Philips Medical Systems, Andover, MA,

USA) with an X7-2t probe. All postoperative images were acquired after cardiopulmonary bypass was stopped during the surgical procedure. Electrocardiographically gated full-volume or 3D zoom images were acquired over four cardiac cycles (Fig. 1a).

## Measurements

We analyzed the geometry of the two types of rings using REAL VIEW 3D analysis software (YD Co., Ltd., Nara, Japan) [7]. We manually marked 32 points on images of implanted mitral annuloplasty rings with 16 rotational sections on the center of the mitral valve (Fig. 1b). The software automatically determined the mitral annular fitting model and calculated the annular area, circumference, antero-posterior diameter, medio-lateral diameter, and height (Fig. 1c). Ring height and ellipticity were measured at four evenly spaced phases during both systole and diastole (eight phases per cardiac cycle) and changes in ring height and ellipticity in one cardiac cycle calculated. Ring height was defined as the shortest distance between two lines in the 3D field (one line passed through the two highest points of the ring, and the other passed through the two lowest points of the ring when the annuloplasty ring

**Table 1** Patient characteristics

	Total $n = 31$	Cosgrove $n = 11$	Memo 3D $n = 20$	<i>p</i> value
Age (years)	$67.2 \pm 15.4$	$65.4 \pm 15.7$	$68.3 \pm 15.1$	0.53
Sex (men %)	48.4	45.5	50.0	0.89
BSA (m <sup>2</sup> )	$1.60 \pm 0.23$	$1.69 \pm 0.23$	$1.56 \pm 0.23$	0.19
Etiology of mitral regurgitation				
Prolapse (%)	77.4	100.0	70.0	0.066
Annular dilatation (%) (without prolapse)	16.1	0.0	25.0	0.13
Infective endocarditis (%) (with or without prolapse)	22.6	18.2	25.0	0.99
Comorbidity				
Aortic stenosis (%)	6.7	0.0	10.0	0.53
Aortic regurgitation (%)	9.7	0.0	15.0	0.54
Tricuspid regurgitation (%)	25.8	18.2	30.0	0.68
Coronary artery disease (%)	9.7	9.1	10.0	0.58
Echocardiographic parameters				
LVDd (mm)	$54.1 \pm 6.8$	$53.1 \pm 4.0$	$54.7 \pm 7.9$	0.63
LVDs (mm)	$34.2 \pm 7.0$	$30.9 \pm 4.2$	$36.0 \pm 7.5$	0.062
EF (%)	$65.5 \pm 11.5$	$71.5 \pm 4.0$	$62.1 \pm 11.1$	0.012
LAD (mm)	$46.5 \pm 10.8$	$43.5 \pm 4.5$	$48.2 \pm 12.7$	0.2
TR-PG (mmHg)	$35.2 \pm 15.8$	$33.5 \pm 11.7$	$36.2 \pm 17.6$	0.92
Ring size (mm)	$29.0 \pm 1.5$	$28.9 \pm 1.0$	$29.0 \pm 1.7$	0.97

Values are expressed as mean  $\pm$  standard deviation unless otherwise indicated

BSA body surface area, Cosgrove Cosgrove-Edwards annuloplasty rings, EF ejection fraction, LAD left atrial dimension, LVDd left ventricular end-diastolic dimension, LVDs left ventricular end-systolic dimension, Memo 3D Sorin Memo-3D annuloplasty rings, TR-PG pressure gradient calculated from Doppler velocity of tricuspid regurgitation

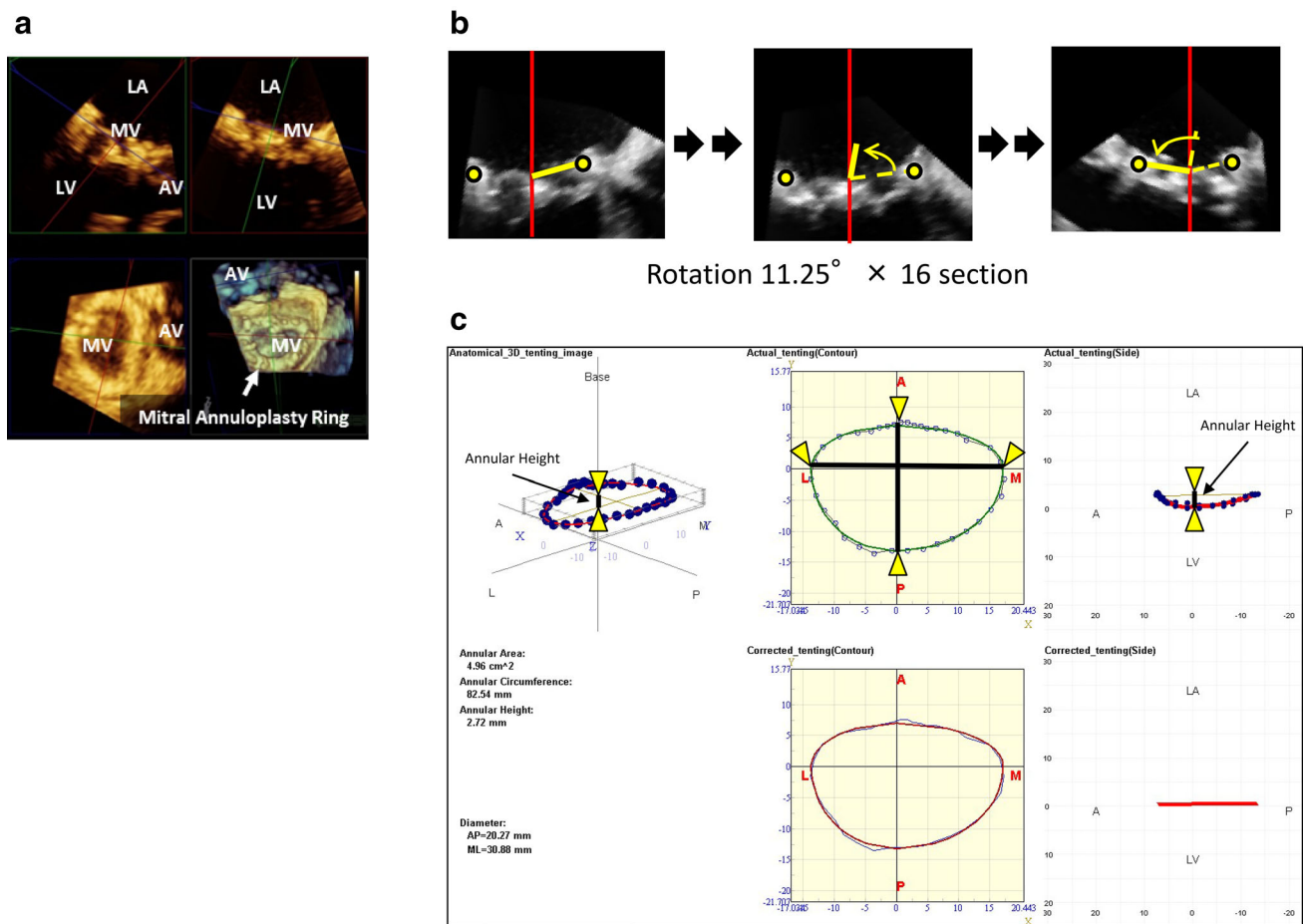


**Fig. 1** Imaging findings, annular fitting model and annular height. **a** Real-time three-dimensional trans-esophageal echocardiography images of mitral annuloplasty ring after mitral plasty. AV aortic valve; LA left atrium; LV left ventricle; MV mitral valve. **b** Images of 32 manually marked points on mitral annuloplasty ring with 16 rotational

sections on center of mitral valve using REAL VIEW software. **c** Results of analysis for determining annular fitting model and calculating annular height, AP (antero-posterior) diameter, and ML (medio-lateral) diameter

was laid on a hypothetical plane surface; Fig. 1c). The mean ring height was the average ring height at all eight phases during one cardiac cycle in each patient. A change in ring height was defined as the maximum difference in ring height during one cardiac cycle. Ring ellipticity was defined as the ratio (%) of the antero-posterior to the medio-lateral diameter of the ring (Fig. 1c). Mean ring ellipticity was defined as the average ring ellipticity of all eight phases during one cardiac cycle. A change in ring ellipticity was defined as the maximum difference in ring ellipticity during one cardiac cycle.

### Statistical analysis

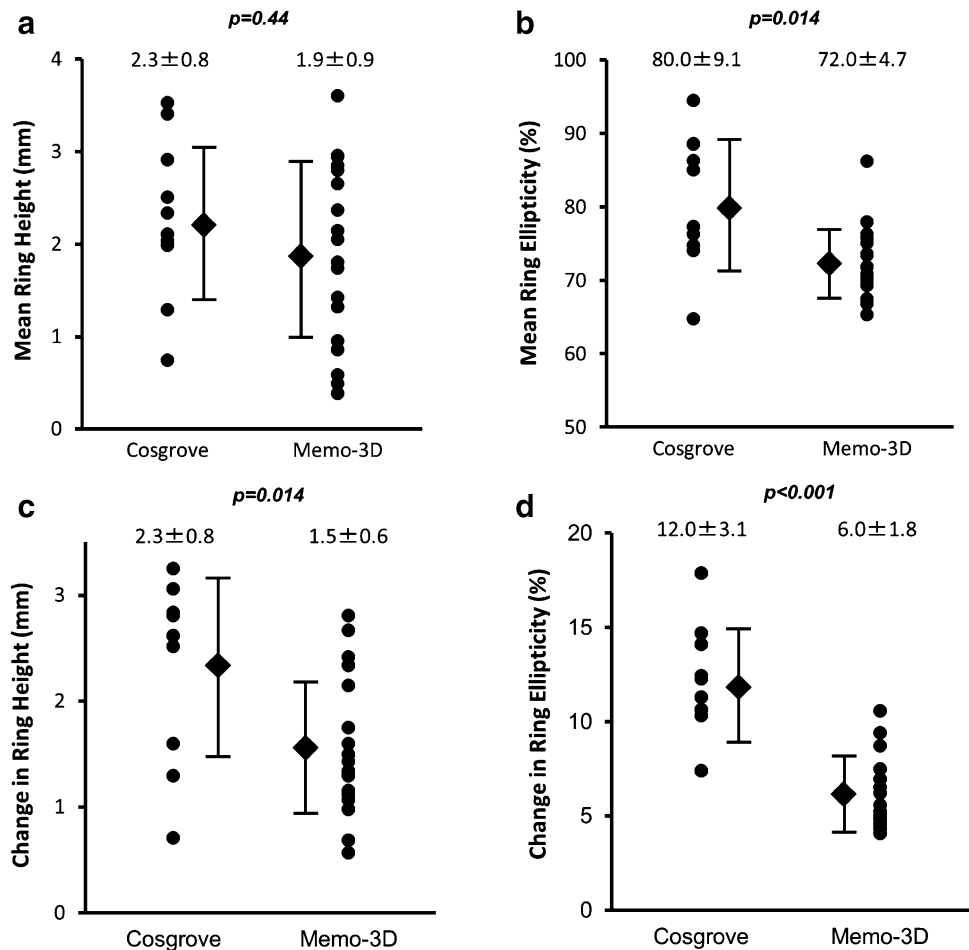
Unless otherwise indicated, values are expressed as means  $\pm$  standard of deviation (SD). Continuous variables were compared using the Mann–Whitney *U* test and categorical data between the Cosgrove and Memo-3D groups were compared using the Chi square test. Associations

between the characteristics of the patients and ring height and ellipticity were evaluated using multivariable linear regression analysis that included variables that were significant in univariate linear regression analyses. A *p* value of  $<0.05$  was taken as significant and all data were analyzed using JMP Pro 11.2.0 software (SAS Institute, Inc., Cary, NC, USA.).

### Results

The characteristics of the patients implanted with Cosgrove and Memo-3D annuloplasty rings were similar except for ejection fraction ( $71.5 \pm 4.0$  vs.  $62.1 \pm 11.1$  %,  $p = 0.012$ ; Table 1). Mean ring height was comparable between the groups ( $2.3 \pm 0.8$  and  $1.9 \pm 0.9$  mm,  $p = 0.44$ ; Fig. 2a), but mean ring ellipticity was larger in the Cosgrove, than in the Memo-3D group ( $80.0 \pm 9.1$  and  $72.0 \pm 4.7$  %,  $p = 0.014$ ; Fig. 2b). Ring height and

**Fig. 2** Changes in mean ring height and ellipticity. Mean ring height (a) and ellipticity (b) in both groups. Changes in ring height (c) and ellipticity (d) in both groups. Values are expressed as mean  $\pm$  standard deviation



ellipticity changed more in the Cosgrove, than in the Memo-3D group ( $2.3 \pm 0.8$  and  $1.5 \pm 0.6$  mm,  $p = 0.014$  and  $12.0 \pm 3.1$  and  $6.0 \pm 1.8$  %,  $p < 0.001$ , respectively; Fig. 2c, d, respectively). Linear regression analyses did not significantly associate patient characteristics and ring type with mean ring height (Table 2). Multivariable linear regression analysis significantly associated body surface area (BSA; standardized  $\beta = 0.35$ ,  $p = 0.017$ ), coronary artery disease (standardized  $\beta = 0.41$ ,  $p = 0.005$ ) and ring type (standardized  $\beta = 0.42$ ,  $p = 0.005$ ) with mean ring ellipticity (Table 2). Univariate linear regression analysis significantly associated left ventricular end-systolic dimension (LVDs; standardized  $\beta = -0.4$ ,  $p = 0.028$ ), ejection fraction (EF) (standardized  $\beta = 0.36$ ,  $p = 0.045$ ), and ring type (standardized  $\beta = 0.48$ ,  $p = 0.007$ ) with changes in ring height, but multivariable analysis significantly associated only ring type with changes in ring height (standardized  $\beta = 0.39$ ,  $p = 0.038$ ) (Table 3). Univariate linear regression analysis significantly associated BSA (standardized  $\beta = 0.38$ ,  $p = 0.037$ ), prolapse (standardized  $\beta = 0.45$ ,  $p = 0.012$ ), annular dilation (standardized  $\beta = -0.4$ ,  $p = 0.024$ ), and ring type (standardized

$\beta = 0.77$ ,  $p < 0.001$ ) with changes in ring ellipticity, but multivariable analysis significantly associated only ring type with changes in ring ellipticity (standardized  $\beta = 0.66$ ,  $p < 0.001$ ; Table 3).

## Discussion

A comparison of 3D-geometric changes between implanted Cosgrove Memo-3D rings during one cardiac cycle using 3D-TEE after mitral plasty revealed that the Cosgrove ring was more flexible, whereas the Memo-3D ring maintained the elliptical shape more effectively.

The mitral annulus is shaped like a horse saddle [1, 8], which is thought to help reduce stress on the mitral leaflets [9–11]. However, because significant MR could cause the mitral annulus to lose the saddle shape [12, 13], artificial rings for mitral annuloplasty should also be saddle-shaped.

The 3D saddle shape of the mitral annulus changes during the cardiac cycle. The height increases during systole, according to biplane videofluoroscopy analysis of radiopaque markers sewn onto the mitral annuli of sheep

**Table 2** Linear regression analyses of mean ring height and ellipticity

	Mean ring height				Mean ring ellipticity			
	Univariate		Multivariable		Univariate		Multivariable	
	Standardized $\beta$ coefficient	<i>p</i> value	Standardized $\beta$ coefficient	<i>p</i> value	Standardized $\beta$ coefficient	<i>p</i> value	Standardized $\beta$ coefficient	<i>p</i> value
Age (years)	−0.026	0.89			−0.12	0.52		
Sex (men)	−0.35	0.052			−0.24	0.19		
BSA (m <sup>2</sup> )	0.32	0.079			0.43	0.016	0.35	0.017
Etiology of mitral regurgitation								
Prolapse	−0.21	0.26			0.23	0.22		
Annular dilation (without prolapse)	0.28	0.12			−0.25	0.18		
Infective endocarditis (with or without prolapse)	−0.16	0.4			0.067	0.72		
Comorbidity								
Aortic stenosis	0.22	0.25			−0.13	0.5		
Aortic regurgitation	0.013	0.95			0.004	0.98		
Tricuspid regurgitation	0.33	0.067			0.044	0.81		
Coronary artery disease	−0.15	0.42			0.37	0.039	0.41	0.005
Echocardiographic parameters								
LVDd (mm)	−0.13	0.5			0.26	0.15		
LVDs (mm)	−0.046	0.8			0.17	0.35		
EF (%)	−0.083	0.66			−0.005	0.98		
LAD (mm)	0.071	0.7			0.001	0.99		
TR-PG (mmHg)	−0.066	0.72			0.087	0.64		
Ring size (mm)	−0.001	0.99			−0.012	0.95		
Ring type (Cosgrove)	0.19	0.3			0.51	0.003	0.42	0.005

BSA body surface area, *Cosgrove* Cosgrove-Edwards annuloplasty rings, *EF* ejection fraction, *LAD* left atrial dimension, *LVDd* left ventricular end-diastolic dimension, *LVDs* left ventricular end-systolic dimension, *Memo 3D* Sorin Memo-3D annuloplasty rings, *TR-PG* pressure gradient calculated from Doppler velocity of tricuspid regurgitation

[14, 15]. Some investigators found using 3D-trans thoracic echocardiography that the saddle height of the mitral annulus in humans peaks during early systole and flattens during late systole [4, 16]. Others have found using 3D-TEE that the mitral annulus saddle height peaks at mid-systole and flattens during late diastole [5]. This discrepancy might be due to the different imaging modalities used to assess mitral annulus motion. We found that mean ring height in all patients peaked at mid-systole and flattened at late diastole, which was compatible with 3D-TEE findings reported by others.

How the shape of implanted mitral annuloplasty rings changes during the cardiac cycle has not been fully investigated. A comparison of flexible Duran and Tailor semi-closed rings during physiological changes using biplane cinefluoroscopy has shown that annular height dynamics were preserved in the Tailor rings, and damped in the Duran ring [17]. On the other hand, 3D-TEE has not identified any differences in geometric dynamics between anterior and posterior flexible rings [18]. The present study

using 3D-TEE uncovered differences between Cosgrove and Memo-3D rings in humans.

The Memo-3D ring is semi-rigid and it should restore the geometry of the mitral annulus and leaflet and to adjust to mitral annulus dynamics during the cardiac cycle [19, 20]. Ryomoto et al. reported that the saddle height of the Memo-3D ring is lower than that of the Carpentier Edwards Physio II ring (Edwards Lifesciences, Irvine, CA, USA) and the St. Jude Medical Rigid Saddle Ring (St. Jude Medical, St. Paul, MN, USA). However, the rate at which the saddle height of the Memo-3D increased from end diastole to end systole was larger than that of Physio II ring and Rigid Saddle Ring [21]. This suggests that the saddle height of the Memo-3D ring is more flexible than that of the Rigid Saddle Ring and the semi-rigid Physio II ring. We calculated the annular height commissure width ratio (AHCWR) to compare the present findings with those of Ryomoto. The maximum AHCWR of the Memo-3D and the change of AHCWR during one cardiac cycle compared with the findings of Ryomoto during one cardiac cycle

**Table 3** Linear regression analyses of changes in ring height and ellipticity

	Change in ring height				Change in ring ellipticity			
	Univariate		Multivariable		Univariate		Multivariable	
	Standardized $\beta$ coefficient	<i>p</i> value	Standardized $\beta$ coefficient	<i>p</i> value	Standardized $\beta$ coefficient	<i>p</i> value	Standardized $\beta$ coefficient	<i>p</i> value
Age (years)	−0.27	0.14			−0.24	0.19		
Sex (men)	0.1	0.58			−0.1	0.59		
BSA (m <sup>2</sup> )	0.017	0.93			0.38	0.037	0.16	0.19
Etiology of mitral regurgitation								
Prolapse	0.23	0.21			0.45	0.012	0.19	0.49
Annular dilation (without prolapse)	−0.16	0.4			−0.4	0.024	0.016	0.95
Infective endocarditis (with or without prolapse)	−0.32	0.082			−0.11	0.55		
Comorbidity								
Aortic stenosis	−0.2	0.29			−0.24	0.19		
Aortic regurgitation	−0.3	0.1			−0.24	0.19		
Tricuspid regurgitation	−0.16	0.39			−0.16	0.39		
Coronary artery disease	0.3	0.11			−0.072	0.7		
Echocardiographic parameters								
LVDd (mm)	−0.21	0.25			0.055	0.77		
LVDs (mm)	−0.4	0.028	−0.26	0.35	−0.18	0.33		
EF (%)	0.36	0.045	0.006	0.98	0.29	0.11		
LAD (mm)	−0.32	0.081			−0.12	0.51		
TR-PG (mmHg)	−0.12	0.53			−0.003	0.99		
Ring size (mm)	−0.041	0.83			0.03	0.87		
Ring type (Cosgrove)	0.48	0.007	0.39	0.038	0.77	<0.001	0.66	<0.001

BSA body surface area, *Cosgrove* Cosgrove-Edwards annuloplasty rings, *EF* ejection fraction, *LAD* left atrial dimension, *LVDd* left ventricular end-diastolic dimension, *LVDs* left ventricular end-systolic dimension, *Memo 3D* Sorin Memo-3D annuloplasty rings, *TR-PG* pressure gradient calculated from Doppler velocity of tricuspid regurgitation

were  $8.8 \pm 3.0$  vs.  $13.6 \pm 3.0$ , and  $5.3 \pm 2.4$  vs.  $5.1 \pm 2.3$  %, respectively. Although we found a smaller maximal AHCWR at end-systole than Ryomoto, changes in AHCWR were similar.

The Cosgrove ring is semi-closed, and its geometry and dynamics correspond to those of the natural mitral annulus. The present study found that the mean saddle height was similar between the Memo-3D and Cosgrove rings. This suggests that the Memo-3D can distort to fit the original mitral annulus after implantation because the Memo-3D is flat and planar before implantation. Our results also showed that mean annular ellipticity was smaller for the Memo-3D than the Cosgrove ring. Because ring ellipticity is defined as the ratio of the antero-posterior to the medio-lateral diameter, a larger ellipse means a more precise circle. Therefore, the Memo-3D ring was more elliptical than the Cosgrove ring and thus might help to maintain coaptation of the mitral leaflets during systole. However, ring type, BSA and coronary artery disease can affect mean ring ellipticity. We found that the standardized  $\beta$  coefficient in multivariable linear regression analysis was the highest for

ring type among these variables. Coronary artery disease might have affected mean ring ellipticity because of left ventricular asynergy. On the other hand, changes in saddle height and annular ellipticity during the cardiac cycle were larger for the Cosgrove, than the Memo-3D ring, and multivariable linear regression analysis significantly associated these with only ring type. Therefore, the Cosgrove ring was deemed appropriate in terms of tracking physiological mitral annular dynamics.

Whether flexible or rigid annuloplasty rings are more effective has not been determined. Flexible rings are considered suitable changes for mitral annulus geometric during the cardiac cycle. Okada et al. reported that the mitral annulus area was more variable with the flexible, than the rigid ring during the cardiac cycle. They also reported that left ventricular fractional shortening and peak velocity at peak exercise was better for the flexible, than the rigid ring [22]. Conversely, Chang et al. found no significant differences in eight-year freedom from recurrence of significant MR, left ventricular systolic function, and post-operative survival between flexible and rigid rings

[23]. Silberman et al. found a better postoperative MR grade and tricuspid regurgitant pressure gradient in ischemic MR with a rigid, than a flexible mitral annuloplasty ring [24]. Maintaining the ideal saddle shape might be more important than mitral annular flexibility for successful mitral plasty.

Collectively, rings with optimal stability and a flexible saddle shape should be ideal. From this perspective, a “semi-rigid” ring might be preferable. We found a similar mean saddle height between the Cosgrove and Memo-3D rings, but the Cosgrove rings were closer to precise circles and more flexible than the Memo-3D rings. That is, the saddle height and elliptical shape of the Memo-3D rings were better maintained, but with variability. The dynamics and operative outcomes of semi-rigid annuloplasty rings have not been fully investigated and thus further study is needed. We plan to assess the long-term results of the ring types used for mitral plasty and to consider the influence of saddle shape flexibility and elliptical shape stability.

## Limitations

This study of a small sample of patients was not randomized with regard to ring selection, did not include consecutive patients, and was not blinded to the echocardiographic findings. The results might have been affected by ring selection bias or differences in preoperative mitral annular ellipticity or saddle height, which we could not investigate. The intraoperative timing of 3D-TEE imaging might not reflect physiological hemodynamics, even though images were obtained after terminating cardiopulmonary bypass. Although significantly different between the groups, multivariable linear regression analysis did not significantly associate EF with mean ring height or ellipticity, or with changes in ring height and ellipticity.

## Conclusions

The Cosgrove annuloplasty ring is more flexible, which might allow better tracking of geometric changes in saddle-shape during the cardiac cycle. The Memo-3D ring maintains the elliptical shape of the mitral annulus during the cardiac cycle better.

**Acknowledgments** We are Grateful Dr. Shiro Yamachika and the sonographers at the ultrasound imaging center in our hospital for invaluable assistance.

## Compliance with ethical standards

**Conflict of interest disclosure statement** Akira Tsuneto received a research Grant from Japan Lifeline Co., Ltd. (Tokyo, Japan). Koji

Maemura received lecture fees from MSD Co., Ltd. (Tokyo, Japan). None of the other authors has any conflicts of interest to declare.

## References

1. Levine RA, Handschumacher MD, Sanfilippo AJ, Hagege AA, Harrigan P, Marshall JE, et al. Three-dimensional echocardiographic reconstruction of the mitral valve, with implications for the diagnosis of mitral valve prolapse. *Circulation*. 1989;80:589–98.
2. Ryan LP, Jackson BM, Enomoto Y, Parish L, Plappert TJ, St John-Sutton MG, et al. Description of regional mitral annular nonplanarity in healthy human subjects: a novel methodology. *J Thorac Cardiovasc Surg*. 2007;134:644–8.
3. Daimon M, Saracino G, Fukuda S, Koyama Y, Kwan J, Song JM, et al. Dynamic change of mitral annular geometry and motion in ischemic mitral regurgitation assessed by a computerized 3D echo method. *Echocardiography*. 2010;27:1069–77.
4. Kwan J, Qin JX, Popovic ZB, Agler DA, Thomas JD, Shiota T. Geometric changes of mitral annulus assessed by real-time 3-dimensional echocardiography: becoming enlarged and less nonplanar in the anteroposterior direction during systole in proportion to global left ventricular systolic function. *J Am Soc Echocardiogr*. 2004;17:1179–84.
5. Levack MM, Jassar AS, Shang EK, Vergnat M, Woo YJ, Acker MA, et al. Three-dimensional echocardiographic analysis of mitral annular dynamics: implication for annuloplasty selection. *Circulation*. 2012;126:S183–8.
6. Miura T, Ariyoshi T, Tanigawa K, Matsukuma S, Yokose S, Sumi M, et al. Technical aspects of mitral valve repair in Barlow’s valve with prolapse of both leaflets: triangular resection for excess tissue, sophisticated chordal replacement, and their combination (the restoration technique). *Gen Thorac Cardiovasc Surg*. 2015;63:61–70.
7. Pressman GS, Movva R, Topilsky Y, Clavel MA, Saldanha JA, Watanabe N, et al. Mitral annular dynamics in mitral annular calcification: a three-dimensional imaging study. *J Am Soc Echocardiogr*. 2015;28:786–94.
8. Gorman JH 3rd, Gupta KB, Streicher JT, Gorman RC, Jackson BM, Ratcliffe MB, et al. Dynamic three-dimensional imaging of the mitral valve and left ventricle by rapid sonomicrometry array localization. *J Thorac Cardiovasc Surg*. 1996;112:712–26.
9. Salgo IS, Gorman JH, Gorman RC, Jackson BM, Bowen FW, Plappert T, et al. Effect of annular shape on leaflet curvature in reducing mitral leaflet stress. *Circulation*. 2002;106:711–7.
10. Jimenez JH, Liou SW, Padala M, He Z, Sacks M, Gorman RC, et al. A saddle-shaped annulus reduces systolic strain on the central region of the mitral valve anterior leaflet. *J Thorac Cardiovasc Surg*. 2007;134:1562–8.
11. Padala M, Hutchison RA, Croft LR, Jimenez JH, Gorman RC, Gorman JH 3rd, et al. Saddle shape of the mitral annulus reduces systolic strains on the P2 segment of the posterior mitral leaflet. *Ann Thorac Surg*. 2009;88:1499–504.
12. Jassar AS, Vergnat M, Jackson BM, McGarvey JR, Cheung AT, Ferrari G, et al. Regional annular geometry in patients with mitral regurgitation: implications for annuloplasty ring selection. *Ann Thorac Surg*. 2014;97:64–70.
13. Lee AP, Hsiung MC, Salgo IS, Fang F, Xie JM, Zhang YC, et al. Quantitative analysis of mitral valve morphology in mitral valve prolapse with real-time 3-dimensional echocardiography: importance of annular saddle shape in the pathogenesis of mitral regurgitation. *Circulation*. 2013;127:832–41.
14. Itoh A, Ennis DB, Bothe W, Swanson JC, Krishnamurthy G, Nguyen TC, et al. Mitral annular hinge motion contribution to

- changes in mitral septal-lateral dimension and annular area. *J Thorac Cardiovasc Surg.* 2009;138:1090–9.
15. Rausch MK, Bothe W, Kvitting JP, Swanson JC, Ingels NB Jr, Miller DC, et al. Characterization of mitral valve annular dynamics in the beating heart. *Ann Biomed Eng.* 2011;39:1690–702.
  16. Topilsky Y, Vaturi O, Watanabe N, Bichara V, Nkomo VT, Michelena H, et al. Real-time 3-dimensional dynamics of functional mitral regurgitation: a prospective quantitative and mechanistic study. *J Am Heart Assoc.* 2013;2:e000039.
  17. Dagum P, Timek T, Green GR, Daughters GT, Liang D, Ingels NB Jr, et al. Three-dimensional geometric comparison of partial and complete flexible mitral annuloplasty rings. *J Thorac Cardiovasc Surg.* 2001;122:665–73.
  18. Owais K, Kim H, Khabbaz KR, Bergman R, Matyal R, Gorman RC, et al. In-vivo analysis of selectively flexible mitral annuloplasty rings using three-dimensional echocardiography. *Ann Thorac Surg.* 2014;97:2005–10.
  19. Bruno PG, Leva C, Santambrogio L, Lazzarini I, Musazzi G, Del Rosso G, et al. Early clinical experience and echocardiographic results with a new semirigid mitral annuloplasty ring: the Sorin Memo 3D. *Ann Thorac Surg.* 2009;88:1492–8.
  20. Santarpino G, Pfeiffer S, Fischlein T. First-in-man implantation of a Sorin Memo 3D ring: mitral annular flexibility is still preserved at 5 years of follow-up! *Int J Cardiol.* 2012;159:e23–4.
  21. Ryomoto M, Mitsuno M, Yamamura M, Tanaka H, Fukui S, Tsujiya N, et al. Is physiologic annular dynamics preserved after mitral valve repair with rigid or semirigid ring? *Ann Thorac Surg.* 2014;97:492–7.
  22. Okada Y, Shomura T, Yamaura Y, Yoshikawa J. Comparison of the Carpentier and Duran prosthetic rings used in mitral reconstruction. *Ann Thorac Surg.* 1995;59:658–62 (**discussion 62–3**).
  23. Chang BC, Youn YN, Ha JW, Lim SH, Hong YS, Chung N. Long-term clinical results of mitral valvuloplasty using flexible and rigid rings: a prospective and randomized study. *J Thorac Cardiovasc Surg.* 2007;133:995–1003.
  24. Silberman S, Klutstein MW, Sabag T, Oren A, Fink D, Merin O, et al. Repair of ischemic mitral regurgitation: comparison between flexible and rigid annuloplasty rings. *Ann Thorac Surg.* 2009;87:1721–6 (**discussion 6–7**).